Mapana – Journal of Sciences
2025, Vol. 24, No. 4, 53-67
ISSN 0975-3303 | https://doi.org/10.12723/mjs.72.4

Effect of Synthetic and Natural Chelating Agent on Yttrium Iron Garnet (YIG) Nanocrystalline Powder via Sol Gel Method

M. Asisi Janifer*, S. Anand†, M. Muralidharan‡, M. Senthuuran§ and S. Pauline*

Abstract

The influence of synthetic and natural chelating agents on the structure, morphology, and magnetic properties of pure Yttrium Iron Garnet ($Y_3Fe_5O_{12}$) is examined. YIG samples are manufactured utilising the synthetic chelating agent citric acid and the natural chelating agent lemon extract at varying temperatures. The generated samples are examined by X-ray Diffraction analysis (XRD). The X-ray Diffraction Pattern (XRD) revealed the garnet phase of nano ferrites at elevated temperatures. The morphological characteristics and elemental composition of the YIG samples are examined using High-Resolution Scanning Electron Microscopy (HRSEM) and Energy-dispersive X-ray Spectroscopy (EDAX), respectively. Metal oxide vibrations (M-O) and active Raman modes are analysed using Fourier Transform Infrared spectroscopy (FTIR) and Raman spectroscopy. The room-temperature magnetic characteristics of YIG samples are examined using a Vibrating Sample Magnetometer (VSM). The dielectric constant and dielectric loss of the nanomaterial are examined across multiple frequencies at varied temperatures.

Keywords: Garnet, Chelating agents, HRSEM, VSM, Dielectric studies.

* Department of Physics, Stella Maris College (Autonomous), Chennai -600086, India; asisijanifer@stellamariscollege.edu.in

† Department of Polymer Science and Engineering Korea National University, Chungju 27469, Republic of Korea; asisijanifer@stellamariscollege.edu.in

‡ *Department of Physics, S. A. Engineering College, Chennai-600077, India;* asisijanifer@stellamariscollege.edu.in

§ Department of Physics, Loyola College, Chennai -600034, India; asisijanifer@stellamariscollege.edu.in

1. Introduction

Ferrites have captivated researchers significantly due to their relevance in technological applications. These applications encompass microwave devices, ferrofluids, drug delivery, and high-density information storage due to their high resistivity, narrow linewidth in ferromagnetic resonance, magneto-optical properties, low eddy current losses, moderate thermal expansion coefficient, and distinctive electric and magnetic properties [1]. The need for technical applications of soft magnetic materials is consistently rising due to their exceptional electromagnetic characteristics. The low electrical conductivity and minimal dielectric losses of ferrites render them exceptional for microwave devices. Ferrites are classed based on their crystal structure. 1) Spinel Ferrite; 2) Garnet; 3) Orthoferrite; 4) Hexagonal Ferrites. Yttrium iron garnet ($Y_3Fe_5O_{12}$), a notable member of the garnet family, is a recognised rare earth garnet ferrite that has garnered significant interest owing to its technological relevance in diverse applications, including isolators, circulators, high-quality filters, phase shifters, and various electronic and magnetic optical devices [2]. The YIG crystal structure is cubic and classified under the space group Oh10 - Ia3d, where magnetic Fe 3+ ions are situated at octahedral 16(a) and tetrahedral 24(d) sites, while non-magnetic Y 3+ ions are located at dodecahedral 24(c) sites [3]. Garnet ferrites exhibit superior chemical stability compared to spinel ferrites due to the complete occupation of all sites by metal cations in well-structured garnets [4]. The performance and application of magnetic materials are mostly influenced by their dielectric and magnetic properties; thus, the electric and magnetic characteristics of nanocrystalline Yttrium iron garnet (YIG) have been effectively examined for frequency-dependent applications.

Numerous publications have been published on the synthesis of YIG using various methods, including solid-state reaction, sol-gel, co-precipitation, microemulsion, organic precursor method, mechanochemical, and hydrothermal techniques. The sol-gel approach is an efficient procedure since it facilitates atomic-scale mixing and accelerates the reaction rate, resulting in homogeneous nucleation of magnetic particles at relatively low temperatures [5]. The characteristics of garnet ferrites are significantly influenced by phase development, microstructure, production methods, and sintering temperature [6].

Gelation occurs in the sol-gel process through the utilization of chelating agents and solutions of inorganic metal salts. Upon concentration of these solutions, most metal ions will generate a homogeneous gel to create chelate complexes. Consequently, selecting an appropriate chelating agent is crucial, as it serves complex metal ions, facilitates a stable chemical reaction, and aids in the reduction of non-toxic gases [7,8-9].

Typically, superior outcomes with reduced crystallite sizes are achieved by employing citric acid as a chelating agent. The crystallite size of YIG was reported to be 73 nm at 1150°C via the sol-gel technique [2], whereas the crystallite size of Yttrium iron garnet was noted as 75 nm, synthesised using the sol-gel method with citric acid as a chelating agent [10]. Likewise, [5] and several others typically document the synthesis of YIG by the sol-gel approach utilising citric acid since it effectively chelates metal ions, yielding superior results with smaller crystallite sizes compared to alternative procedures. To the best of our knowledge, the synthesis of YIG with natural lemon extract has not been documented. This research primarily aims to elucidate the properties of nanocrystalline YIG synthesised with natural lemon extract and synthetic citric acid as chelating agents, to investigate the differences in properties conferred by these agents, and to analyse the electric and magnetic characteristics of the resultant YIG for microwave and other applications.

2. Experimental

For the preparation of yttrium iron garnet, yttrium nitrate hexahydrate ($Y(NO_3)_3.6H_2O$, 99.99%) and iron nitrate nonahydrate ($Fe(NO_3)_3.9H_2O$, 99.99%) were taken as starting materials. The stoichiometric compositions of the solution components (fuels and oxidiser) were determined using propellant chemistry principles, with the oxidiser (metal nitrate) to fuel (citric acid) ratio set at unity.

Oxidizing valency of $Y(NO_3)_3.6H_2O$: 1Y = +3, 3N = 0, 9O = -18, 12H = +12, 6O = -12, $Fe(NO_3)_3.9H_2O$: 1Fe = +3, 3N = 0, 9O = -18, 18H = +18, 9O = -18.

Reducing valency of $C_6H_8O_7.H_2O$: 6C = +24, 8H = +8, 7O = -14, 2H = +2, 1O = -2

($\boldsymbol{\varphi e}$) $(O/F) = \frac{3/8\,(-15) + 5/8\,(-15)}{(-1)\,(-18)} = 0.833$ i.e., for every one mole of $Y(NO_3)_3$ and $Fe(NO_3)_3$, 0.833 mol of citric acid is required.

The metal nitrates $Y(NO_3)_3.6H_2O$and $Fe(NO_3)_3.9H_2O$ were dissolved in the aqueous solution of 160 ml of citric acid $C_6H_8O_7.H_2O$, the chelating agent. Metal nitrates and citric acid were kept at a molar ratio of 1:1. For three to four days, the solution was agitated at 310 rpm. With constant stirring, the temperature was raised to 80°C till gel formed. The gel samples were dried for 34 hours at 110°C. Following two to three hours of grinding, the dried powders were annealed for four hours in air at 1150°C. Lemon juice (0.004 mol/L) was used as the chelating agent in the same way, but the temperature was lowered to 1000°C [2].

2.1 Characterization

The crystalline structure and phase identification of the $Y_3Fe_5O_{12}$ samples produced via the sol-gel process at different temperatures were analysed using a Bruker D8 Advance X-ray diffractometer, operated at 40 kV and 30 mA with CuKα radiation (λ = 1.5406 Å). The sample's chemical composition and morphology were analysed using an FEI Quanta FEG 200 High-Resolution Scanning Electron Microscope in conjunction with an Energy Dispersive Spectrum. A Perkin-Elmer spectrometer, model 2000, was employed to obtain Fourier transform infrared (FTIR) spectra ranging from 400 to 4000 cm-1. KBr was utilised to prepare the material in pellet form. Raman spectra were reported using LASER Raman Spectroscopy Analysis. The electric and magnetic properties of the sample were analysed using a Lakeshore model (7407) Vibrating Sample Magnetometer (VSM) and a HIOKI LCR meter.

3. Result And Discussion

3.1. The phase identification of YIG nanoparticles by XRD

Distinct peaks signifying a high degree of crystallinity were seen at temperatures of 1150°C and 1000°C, utilising citric acid and lemon juice as chelating agents, respectively, as illustrated in Fig. 1. Remarkably, all peaks from both reports precisely corresponded with the conventional JCPDS data (75-1852) for Yttrium Iron Garnet. Significantly, at lower temperatures, lemon extract demonstrated the precise garnet phase. The XRD pattern indicated the presence of YIG with the (420) plane when annealed at elevated temperatures of 1150°C using citric acid and 1000°C using lemon extract. The annealing temperature was optimised for citric acid across various temperatures, revealing intriguing phase development in the sample annealed at 650°C using lemon extract, as no peaks were observed for the nanomaterial annealed at that temperature with citric acid. This prompted the research to employ a lower annealing temperature for LJ in comparison to CA.

The average crystallite size and lattice parameter of YIG samples were calculated using the Scherer formula,

$$D = \frac{K\lambda}{\beta \cos\theta}$$

Whereas λ = wavelength of incident radiation, ω =Full width at half maximum (FWHM), K= varies with hkl & crystallite shape equal to 0.89, θ = Bragg's angle.

The crystallite diameters of YIG synthesised at temperatures of 1000°C and 1150°C utilising lemon extract and citric acid are measured at 56.6 nm and 65.5 nm, respectively. At 950°C, the crystallite size was determined to

be 51nm when utilising citric acid, which is comparable to the crystallite size of YIG at 1000°C with lemon juice, so demonstrating the diminished crystallite size when employing lemon juice. The metrics, including X-ray density, specific surface area, and packing factor, evaluated from XRD, are shown in the table. The packing factor (p) is determined by the equation p = D / d, where D represents the average crystallite size and d denotes the interplanar spacing. The specific surface area (SSA) can be determined using the Sauter formula: $S = 6/(D)(\rho_{xrd})$. The computed XRD parameters [11] are displayed in Table 1.

Citric acid (2-hydroxy-1,2,3-propanetricarboxylic acid) is a weak tricarboxylic acid predominantly found in citrus fruits. It is typically regarded as an effective complexing agent due to its ability to form superior homogeneous gels by complexing metals in solution [7]. In comparison to other chelating agents, citric acid showed favourable results with reduced crystallite sizes at low temperatures, while the sizes predominantly remained over 65 nm. This study utilised lemon extract as a substitute for citric acid to synthesise YIG with reduced crystallite size at relatively lower temperatures. Citrus limon Is a member of the citrus family Rutaceae. Lemon juice comprises citric acid along with many other chemical components, including ascorbic acid and flavonoids such as hesperidoside and limocitrin. The predominant misconception regarding citric acid is that it is equivalent to vitamin C. Ascorbic acid is the scientific designation for vitamin C, which is a completely different molecule. The XRD analysis indicated the presence of massive crystallites at elevated temperatures with citric acid serving as the chelating agent. The lemon extract produced a diminished crystallite size of the specific garnet phase at a lower temperature. Consequently, citric acid, vitamin C, and other components in lemon juice provide more carbon for accelerated reactions, thereby facilitating the manifestation of the garnet phase at lower temperatures with diminished crystallite size. No reaction between the initial powders transpired before sintering, nor during sintering at 600°C with citric acid, as corroborated by [12]. Lemon juice exhibited crystallisation at 650°C, accompanied by the secondary phase $YFeO_3$ and the garnet phase $Y_3Fe_5O_{12}$. Clearly, delineated and vibrant garnet peaks are observed devoid of contaminants at elevated temperatures.

Table 1: Parameters calculated from XRD analysis

Parameters	YIG at 1150°C (CA)	YIG at 1000°C (LJ)
$D_{(4\,2\,0)}$ (nm)	65.5	56.8
a (Å)	12.29	12.34
V (Å^3)	1856	1879
ρ XRD(g cm^{-3})	5.28	5.21
S (m^2/g)	17.34	20.20
packing factor (*p*)	23.73	26.95

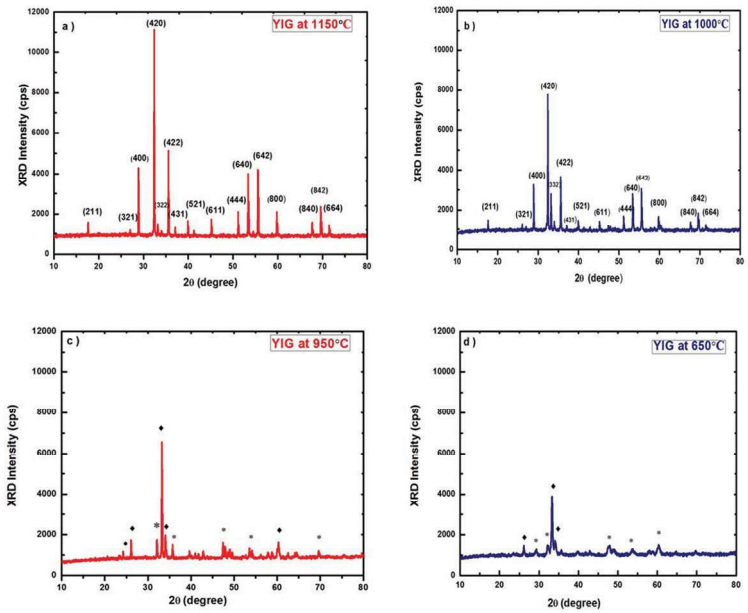

Fig. 1.XRD patterns of the samples a) at 1150°C using CA, b) at 1000°C using LJ, c) at 950°C using CA, d) at 650°C using LJ.[citric acid – CA, lemon juice – LJ]
♦ - $YFeO_3$, ● - Fe_2O_3, * - $Y_3Fe_5O_{12}$

3.2. Morphology of YIG nanoparticles by SEM

The standard SEM micrographs of yttrium iron garnet samples depicted in figures 2a), 2b), 2c), and 2d) exhibit distinctly formed particles devoid of aggregation at elevated temperatures. The sample at 950°C (utilising CA) features indeterminate borders and pores that entirely vanish at elevated temperatures. A well-defined spherical shape with specific aggregation is achieved at a low temperature of 650°C using lemon juice, while no reaction was detected with citric acid at that temperature, as described by [12]. The absence of agglomeration eventually demonstrates the consistency and variations in particle size of samples at 1000°C and 1150°C. The pores in the $Y_3Fe_5O_{12}$ sample inhibit atomic diffusion, hence preventing the formation of solid nanocrystalline powder, as further corroborated by XRD analysis. Changes in the particle size and morphology of the $Y_3Fe_5O_{12}$ samples annealed at elevated temperatures are proven to result from the fragmentation and agglomeration of particles [2]. The SEM images further validate the reduced grain size of YIG utilising lemon extract.

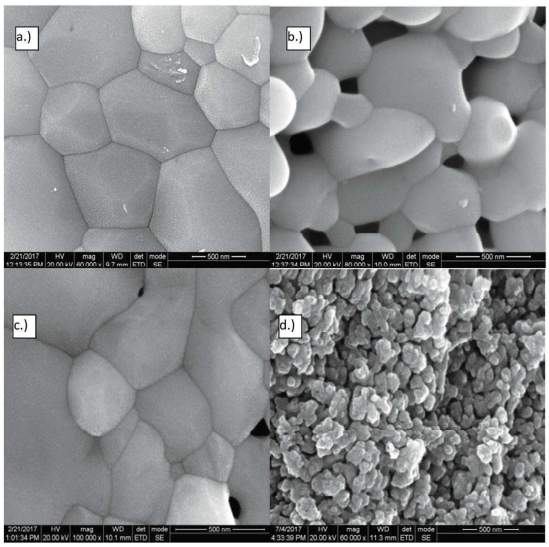

Fig. 2: Scanning Electron Microscopy images of Yttrium iron garnet a) at 1150°C using CA, b)at 1000°C using LJ,c) at 950°C using CA, d) at 650°C using LJ

EDAX Analysis

From the EDX spectrum, it is observed that the sample is devoid of other elements, is shown in Fig. 3.

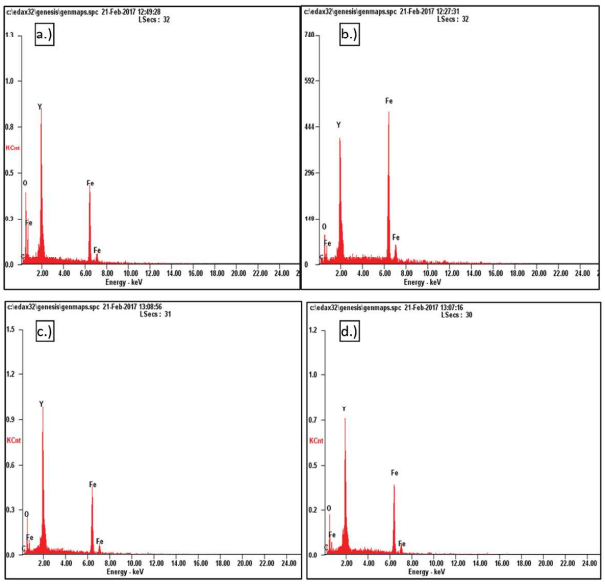

Fig.3: Energy dispersive spectroscopy images of Yttrium iron garnet a) at 1150°C using CA, b)at 1000°C using LJ, c) at 950°C using CA, d) at 650°C using LJ.

3.1. The vibrational spectroscopic analysis of YIG nanoparticles

The FTIR absorbance spectra of YIG produced using citric acid and lemon juice as chelating agents are presented in Fig. 4. YIG samples produced with both chelating agents displayed three asymmetric stretching modes at 649 cm^{-1}, 604 cm^{-1}, 550 cm^{-1}, and 655 cm^{-1}, 604 cm^{-1}, 562 cm^{-1}, respectively. This validated the existence of garnet phases [13]. The band at approximately 2400 cm^{-1} corresponds to the CO_2 contained in the samples. Lemon extract facilitated the manifestation of garnet phases at comparatively lower temperatures. This is because of the higher concentration of carbonyl groups in lemon extract, which facilitates a more rapid reaction for the formation of the precise garnet phase.

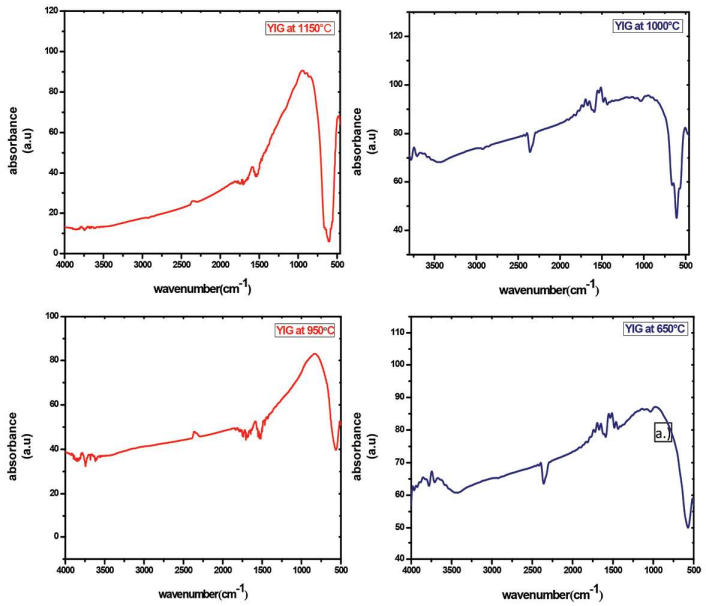

Fig.4: FTIR spectra of Yttrium iron garnet a) at 1150°C using CA, b)at 1000°C using LJ, c) at 950°C using CA, d) at 650°C using LJ.

Raman spectra of YIG synthesised using citric acid and lemon juice as chelating agents are shown in Fig. 5. The prominent peaks at 270 cm^{-1} signify garnet phases and further validate the grain development in the samples. The peaks at 290 cm^{-1}, 220 cm^{-1}, 180 cm^{-1}, and 400 cm^{-1} correspond to Fe_2O_3 and Y_2O_3 molecules, respectively. The signal at 292 cm^{-1} shifts to 270 cm^{-1} at 1150°C, showing that residual Fe_2O_3 is undergoing a reaction to produce YIG. The peaks identified at 160 cm-1, 220 cm-1, 260 cm-1, 340 cm-1, and 370 cm-1 result from the vibrations of the yttrium ion in the YIG sample [14][6]. The garnet peaks are distinctly observed for both chelating agents; however, the influence of the natural chelating agent on garnet displays Raman bands at a somewhat lower temperature, as illustrated in the figure.

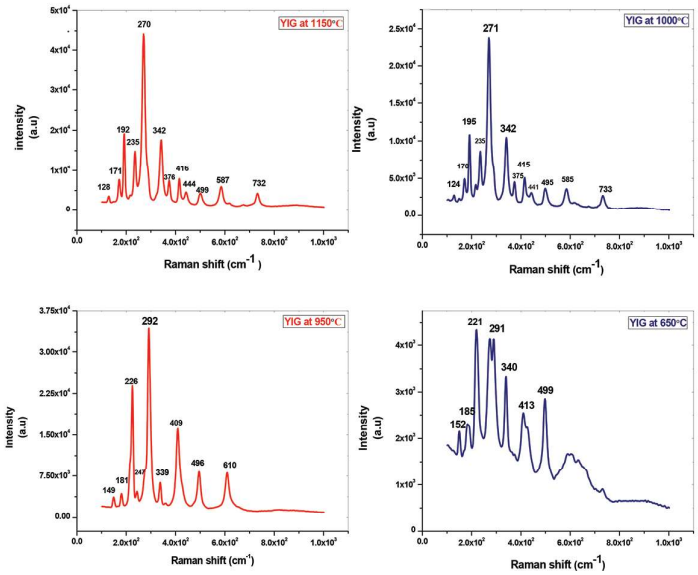

Fig.5: Raman spectra of Yttrium iron garnet a) at 1150°C using CA, b)at 1000°C using LJ, c) at 950°C using CA, d) at 650°C using LJ.

3.3. The dielectric properties of the YIG

The dielectric properties of YIG nanoparticles were examined at various temperatures throughout the frequency range of 50 Hz to 5 MHz utilising an LCR meter. Figure 6 illustrates the dielectric constant, dielectric loss, and alternating current conductivity of dense YIG pellets in relation to frequency and temperature. The electric and dielectric properties are crucial parameters in the design of frequency-dependent devices, influenced by the preparation procedure, sintering temperature, and other conditions. High values of dielectric constant are observed at low frequencies, with a diminishing trend at elevated frequencies. The dependence of ε and tanδ on frequency is characteristic of ferrites. The reduction at elevated frequencies occurs because the oscillation frequency of electric charge carriers cannot sustain the alternation of the applied AC electric field beyond a specific critical frequency [15]. The dielectric constant at low and high frequencies is ascribed to dipolar and interfacial polarisation, which occurs between charges and electronic polarisation, resulting in electron hopping. The elevated dielectric constant is attributable to flaws, voids, morphologies, and dislocations present in these samples [16]. Dielectric tests indicate that the dielectric constant of YIG ranges from 13 to 17 when utilising both chelating agents, as referenced in [17][18]; nevertheless, these investigations documented dielectric constants at temperatures exceeding 1400°C. The dielectric constant (Ɛ') was determined using,

$$\varepsilon' = \frac{C\,d}{\varepsilon_0 A}$$

Where ε_0 the constant of permittivity of free space, d is the pellet thickness, A is the area of cross-section of the pellet, and C is the capacitance. The dielectric loss factor (ε'') and tangent losses tan (δ) are calculated using the relation [19],

$$\varepsilon'' = \varepsilon' * \tan\delta$$

$$\text{Tan}(\delta) = \varepsilon_r''/\varepsilon'$$

The dielectric loss factor graph is analogous to the dielectric constant. The stored energy is described by ε'whereas, the dissipated energy is described by ε''. From the fig it is understood that YIG synthesised using natural lemon extract exhibits dielectric properties at reduced temperature. The parameters calculated from dielectric studies are shown in Table 2.

Table 2. Parameters calculated from dielectric studies

Parameters	YIG at 1150°C (CA)	YIG at 1000°C (LJ)
ε' at 2 kHz	26	21
ε' at 20 kHz	22	18
ε' at 2 MHz	17	13
tanδ at 2 kHz	0.19	0.2
tanδ at 20 kHz	0.01	0.015
tanδ at 2 MHz	0.008	0.005
ε'' at 2 kHz	4.94	4.2
ε'' at 20 kHz	0.22	0.27
ε'' at 2 MHz	0.136	0.065

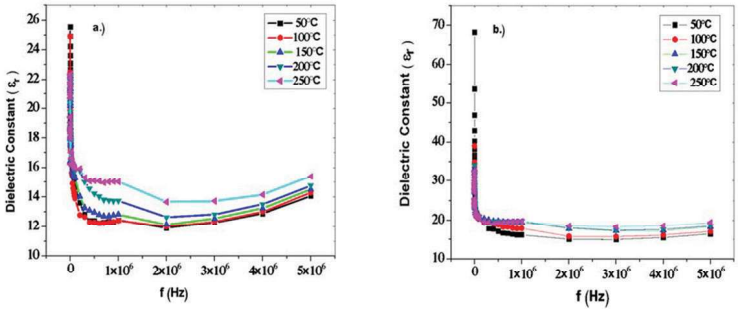

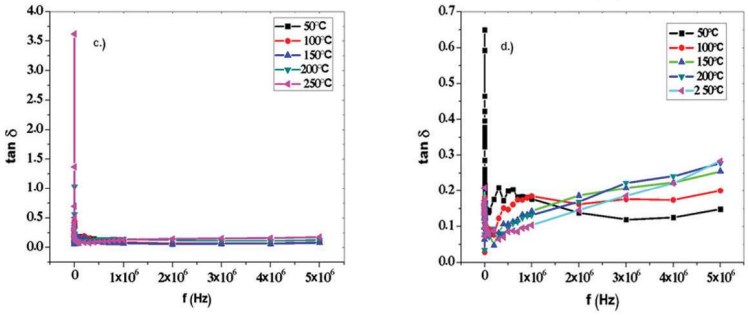

Fig.6: Dielectric constant of Yttrium iron garnet a) at 1150°C using CA, b) at 1000°C using LJ and Dielectric loss of Yttrium iron garnet c) at 1150°C using CA, d) at 1000°C using LJ

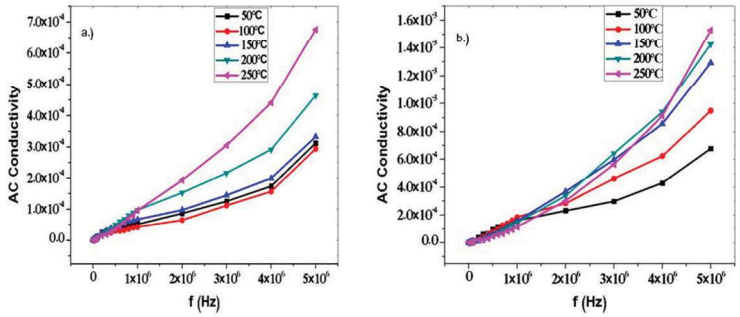

Fig.6.3: a.c conductivity of Yttrium iron garnet a) at 1150°C using CA, b) at 1000°C using LJ

3.2. Magnetic properties of YIG particles

The ferromagnetic properties of YIG samples are assessed up to an applied field of 15 kOe at room temperature utilising VSM. A well-defined M-H hysteresis loop, characterised by a sigmoid form, is exhibited at elevated temperatures, indicating a robust ferromagnetic phase, as illustrated in Fig. 7. The magnetic characteristics derived from lemon extract and citric acid as chelating agents are presented in the table. The Ms value of YIG with citric acid was determined to be 11.6 emu/g, while the Ms value of YIG with lemon extract was 14.2 emu/g. This suggests improved magnetic properties with a natural chelating agent. The saturation magnetisation value Ms and several hundred oersted's of coercivity Hc signify robust magnetism and the soft nature of garnet ferrites. The magnetic characteristics, including saturation, remanence, and squareness ratio, are influenced by both intrinsic factors (composition, synthesis process) and external factors (morphology, porosity) of garnet ferrites. The estimated squareness ratio of approximately 0.75 indicates that garnet ferrites are highly appropriate for microwave applications, particularly in isolators and attenuators. The

minor fluctuations in magnetic remanence (Mr), magnetic saturation (Ms), and coercivity (Hc) for YIG samples may also result from the spin canting effect and the disruption of collinearity [2]. This study concludes that the hysteresis property of YIG is influenced not only by sintering temperature and synthesis methods, as frequently reported, but also by the choice of chelating agent [20-22].

Table 3: Parameters calculated from VSM analysis at room temperature

Parameters	YIG at 1150°C (CA)	YIG at 1000°C (LJ)
$D_{(4\,2\,0)}$ (nm)	65.5	56.6
Ms (emu/g)	11.6	14.2
Mr (emu/g)	8.659	10.64
Mr/Ms	0.740	0.7249
Hc (Oe)	310.81	328.20

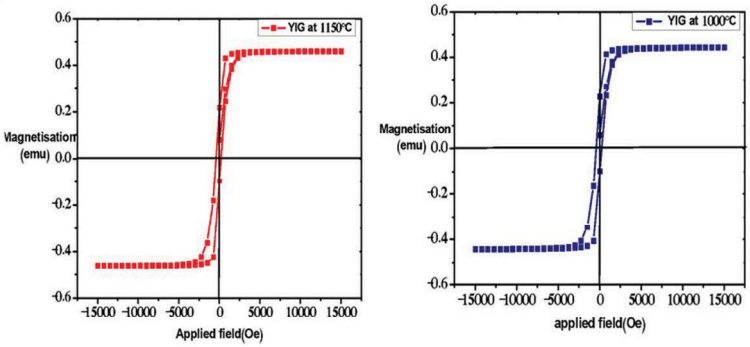

Fig.7: M-H Loops of Yttrium iron garnet samples synthesised a) at 1150°C using CA, b) at 1000°C using LJ

4. Conclusion

The sol-gel method utilising appropriate chelating agents has been identified as a cost-effective and suitable approach for the large-scale production of YIG. The XRD results indicate that the successful formation of a single-phase YIG, characterised by the major peak [420], occurs exclusively at elevated temperatures. The reactions remained incomplete at lower annealing temperatures, and it was only at elevated temperatures that sufficient energy was provided to trigger the reaction and produce nanocrystalline garnet phases. A pure sample of YIG was synthesised utilising the synthetic chelating agent citric acid and the natural chelating agent lemon extract at temperatures of 1150°C and 1000°C, respectively. It is noteworthy that the application of lemon extract as a chelating agent resulted in the formation of single-phase $Y_3Fe_5O_{12}$ (YIG) garnet ferrites, exhibiting a significantly reduced crystallite size at lower temperatures in comparison to the sample synthesised with citric acid. A well-defined structure was clearly observed from HR-SEM, free from other elemental compositions typically regarded

as impurities. The vibrational spectroscopic analysis conducted through FTIR and Raman techniques demonstrated that an increased presence of carbonyl compounds in lemon extract accelerated the reaction, resulting in the production of pure garnet at a comparatively lower temperature. The synthesis conditions have a substantial impact on the structure of garnet phases. The findings from dielectric studies indicate that YIG will be utilised in high-frequency applications because of its reduced dielectric losses at elevated frequencies. Significantly, optimal outcomes are achieved using the natural chelating agent lemon extract at lower temperatures. The magnetic properties were observed to be influenced not only by the intrinsic and extrinsic characteristics of garnet but also by the selection of the chelating agent used in the synthesis process. In conclusion, the natural chelating agent lemon extract demonstrated pure garnet phases at a lower temperature, while YIG has been identified as a promising candidate for frequency-dependent applications and is particularly well-suited for microwave applications, primarily because of its electrical and magnetic properties.

References

[1]. S Nasir, M Anisur Rehman and Muhammad Ali Malik, Structural and dielectric properties of Cr-doped Ni–Zn nanoferrites, Phys. Scr. **83** (2011) 025602 (5pp), doi:10.1088/0031-8949/83/02/025602.

[2]. MajidNiazAkhtar, Muhammad Azhar Khan, Mukhtar Ahmad, G. Murtaza, R.Raza, S. F. Shaukat, M. H. Asif, G. Abbas, M. S. Nazir, M. R.Raza, $Y_3Fe_5O_{12}$ nanoparticulate garnet ferrites: Comprehensive study on the synthesis and characterization fabricated by various routes, Journal of Magnetism and Magnetic Materials, S0304-8853(14)00519-8,doi: 10.1016/j.jmmm.2014.06.004.

[3]. Ftema W. Aldbea, N.B.Ibrahim and M. Yahya,Effect of adding aluminum ion on the structural, optical, electrical and magneticproperties of terbium doped yttrium iron garnet nanoparticles filmsprepared by sol-gel method, Applied Surface Science (2014), doi:10.1016/j.apsusc.2014.10.019.

[4]. Majid Niaz Akhtar, A.B. Sulong, Mukhtar Ahmad, Muhammad Azhar Khan, Akbar Ali, Impacts of Gd-Ce on the Structural, Morphological and Magnetic Properties of Garnet Nanocrystalline Ferrites Synthesized via Sol-gel Route, Journal of Alloys and Compounds, S0925-8388(15)31702-3 doi: 10.1016/j. jallcom.2015.11.146.

[5]. Wang Minqiang , Zhu Xiangying , Wei Xiaoyong, Zhang Liangying& Yao Xi, Preparation and annealing process of $Y_3Fe_5O_{12}$ by sol gel method,Ferroelectrics 5. 2001. Vol. 263. pp. 249-254, doi:10.1080/00150190108008577.

[6]. L. Fernandez-Garcia, M. Suarez, J.L. Menendez, Synthesis of mono and multidomain YIG particles by chemical coprecipitation or ceramic procedure, Journal of Alloys and Compounds 495 (2010) 196–199, doi:10.1016/j. jallcom.2010.01.119.

[7]. P. Vaqueiro and M. A. Lo´pez-Quintela, Influence of Complexing Agents and pH on Yttrium-Iron Garnet Synthesized by the Sol-Gel Method, Chem. Mater. **1997,** 9, 2836-2841.

[8]. Coutinho, D.M. and Verenkar, V.M.S., 2019. Spin canting and surface spin disorder in Ni substituted Co-Cd ferrite nanoparticles synthesized by fuel deficient combustion method. *Journal of Alloys and Compounds*, *782*, pp.392-403.

[9]. Soufi, A., Hajjaoui, H., Elmoubarki, R., Abdennouri, M., Qourzal, S. and Barka, N., 2021. Spinel ferrites nanoparticles: Synthesis methods and application in heterogeneous Fenton oxidation of organic pollutants–A review. *Applied Surface Science Advances*, *6*, p.100145.

[10]. S. Hosseini Vajargah, H.R. Madaah Hosseini , Z.A. Nemati, Synthesis of nanocrystalline yttrium iron garnets by sol–gel combustion process: The influence of pH of precursor solution, Materials Science and Engineering B 129 (2006) 211–215, doi:10.1016/j.mseb.2006.01.014.

[11]. S. Anand, A. Persis Amaliya, M. Asisi Janifer and S. Pauline, Structural, Morphological and Dielectric studies of Zirconium substituted $CoFe_2O_4$ nanoparticles, Modern Electronic Materials, doi:10.1016/j.moem.2017.10.001

[12]. N. Rodziah, M. Hashim, I.R. Idza, I. Ismayadi, A.N. Hapishah, M.A. Khamirul, Dependence of developing magnetic hysteresis characteristics on stages of evolving microstructure in polycrystalline yttrium iron garnet, Applied Surface Science 258 (2012) 2679– 2685, doi:10.1016/j.apsusc.2011.10.117.

[13]. M. Niyaifar , H. Mohammadpour, M. Dorafshani, A. Hasanpour, Size dependence of non-magnetic thickness in YIG nanoparticles, Journal of Magnetism and Magnetic Materials 409 (2016) 104–110, doi.org/10.1016/j. jmmm.2016.02.097.

[14]. Nadeem Nasir, NoorhanaYahya, Muhammad Kashif, HanitaDaud,MajidNiazAkhtar, HasnahMohdZaid, AfzaShafie, and Lee Chaw Teng, Observation of a Cubical-Like Microstructure of Strontium Iron Garnet and Yttrium Iron Garnet Prepared via Sol–Gel Technique, Journal of Nanoscience and Nanotechnology, Vol. 11, 2551–2554, 2011, doi:10.1166/ jnn.2011.2724.

[15]. A.M. abdeen, Dielectric behaviour in Ni—Zn ferrites J. Magn. Magn. Mater. 199 (1999) 121–129. doi:10.1016/S0304-8853(98)00324-2.

[16]. MajidNiazAkhtar, A. Rahman, A.B. Sulong, Muhammad Azhar Khan, Structural, Spectral, Dielectric and Magnetic Properties of Ni0.5MgxZn0.5-xFe2O4 Nanosized ferrites for Microwave absorption and High Frequency Applications, Ceramics InternationalS0272-8842(16)32348-3, doi : 10.1016/j. ceramint.2016.12.081.

[17]. LalithaSirdeshmukh, K Krishna Kumar, S Ballaxman, A Rama Krishna and G Sathaiah, Dielectric properties and electrical conduction in yttrium iron garnet (YIG), Mater. Sci., Vol. 21, No. 3, June 1998, pp. 219-226.

[18]. WanFahmin Faiz Ali,NorazharuddinShahAbdullah, MaslindaKamarudin, MohdFadzilAin, ZainalArifin Ahmad, Sintering and grain growth control of high dense YIG, Ceramics International (2016), .doi:10.1016/j. ceramint.2016.06.004.

[19]. Rabia Ahmad, IftikharHussainGul, Muhammad Zarrar, Humaira Anwar, Muhammad Bilal khan Niazi, Azim Khan, Improved Electrical Properties of Cadmium Substituted Cobalt Ferrites Nano-particles for Microwave Application, Journal of Magnetism and Magnetic MaterialsS0304-8853(15)30885-4,doi: 10.1016/j.jmmm.2015.12.019.

[20]. Majid Niaz Akhtar, A. Rahman, A.B. Sulong, Muhammad Azhar Khan, Structural, Spectral, Dielectric and Magnetic Properties of Ni0.5MgxZn0.5-xFe2O4 Nanosized ferrites for Microwave absorption and High Frequency Applications, Ceramics InternationalS0272-8842(16)32348-3,doi : 10.1016/j.ceramint.2016.12.081.

[21]. SaberE. Mansour, 1 2Monalisa Pattanayak and 2P. L. Nayak, Green Synthesis of Gold Nano Particles VII: Green Synthesis and Characterization of Gold Nano Particles Using the Extract of Lemon (Citrus limon) and Study of its Cytotoxicity Properties, Middle-East Journal of Scientific Research 22 (2): 313-319, 2014,doi: 10.5829/idosi.mejsr.2014.22.02.21877.

[22]. Kristina. Penniston, M.D.,Stephen Y. Nakada, M.D.,Ross P. Holmes and Dean G. Assimos, M.D, Quantitative Assessment of Citric Acid in Lemon Juice, Lime Juice, and Commercially-Available Fruit Juice Products,journal of endourology Volume 22, Number 3, March 2008, doi: 10.1089/end.2007.0304.